Metrol. Meas. Syst., Vol. 30 (2023) No. 1, pp. 117–138
DOI: 10.24425/mms.2023.144401

PAN POLSKA AKADEMIA NAUK

METROLOGY AND MEASUREMENT SYSTEMS

Index 330930, ISSN 0860-8229
www.metrology.wat.edu.pl

M&MS

DEEP LEARNING CLASSIFICATION AND RECOGNITION METHOD FOR MILLING SURFACE ROUGHNESS COMBINED WITH SIMULATION DATA

Lingli Lu[1)], Huaian Yi[1)], Aihua Shu[1)], Jianhua Qin[1)], Enhui Lu[2)]

1) School of Mechanical and Control Engineering, Guilin University of Technology, Guilin, 541006, People's Republic of China (*lulinglilili@163.com*, ✉ *yihuaian@126.com*, *3534497906@qq.com*, *jianhua7@sina.com*)
2) School of Mechanical Engineering, Yangzhou University, Yangzhou, 225009, People's Republic of China (*enhui@yzu.edu.cn*)

Abstract

To address the problem that a deep neural network needs a sufficient number of training samples to have a good prediction performance, this paper firstly used the Z-Map algorithm to generate a simulated profile of the milling surface and construct an optical simulation model of surface imaging to supplement the training sample size of the neural network. Then the Deep CORAL model was used to match the textures of the simulated samples and the actual samples across domains to solve the problem that the simulated samples were not in the same domain as the actual milling samples. Experimental results have shown that high texture matching could be achieved between optical simulation images and actual images, laying the foundation for expanding the actual milled workpiece images with the simulation images. The deep convolutional neural model Xception was used to predict the classification of six classes of data sets with the inclusion of simulation images, and the accuracy was improved from 86.48% to 92.79% compared with the model without the inclusion of simulation images. The proposed method solves the problem of the need for a large number of samples for deep neural networks and lays the foundation for similar methods to predict surface roughness for different machining processes.

Keywords: Milling surface, classification, deep neural network, simulation.

1. Introduction

In the field of modern machinery manufacturing, the surface quality of the workpiece is one of the important indexes to measure manufacturability and affect the performance of the workpiece, and its detection is of great significance in the manufacturing industry [1]. Surface roughness is an important index evaluating the surface quality, so the measurement of the roughness is an essential link in the production process of mechanical parts. The measurement methods of surface roughness can be classified into contact measurement and non-contact measurement. The main disadvantage of the contact measurement method is that the stylus may scratch the

Article history: received June 27, 2022; revised October 17, 2022; accepted November 4, 2022; available online February 2, 2023.

workpiece surface during the measurement process, and it does not support online measurement, resulting in low efficiency [2]. Non-contact measurement methods mainly include optics [3], electronics [4], and machine vision. Among them, the machine vision method is characterized by low cost and high efficiency, so it has attracted wide attention. In machine vision, a corresponding relationship between roughness and evaluation indexes designed by the human is established to realize roughness measurement. Having analyzed the signal-to-noise ratio of roughness images Hamed *et al.* [5] concluded that the roughness of a surface depends on the degree of aggregation of speckle images. Jeyapoovan *et al*. [6] applied biometric identification techniques to characterize processed surface images, using the Euclidean distance and Hamming distance of an image as features for image identification, with the Hamming distance between the reference signal and the test signal being used to estimate the surface roughness class of the test image. Kamguem *et al*. [7] proposed a new method to detect surface roughness based on the image gradient factor. Lu *et al*. [8] proposed a CDSM index. Experimental results proved the feasibility, validity and generality of the proposed index. Yi *et al*. [9] proposed a new roughness measurement method based on color information. By comparing the proposed *CD* index with indexes *Ga*, *En* and *F2*, it can be determined that the *CD* index has a stronger correlation with surface roughness. Yi *et al*. [10] proposed a method to evaluate the surface roughness of grinding based on the detection method of singular value entropy of color images. However, limited by the level of human knowledge, human-designed evaluation indexes fail to meet the requirements of automatic measurement and self-extraction of image features. Therefore, in recent years, many scholars have tried to use deep learning and other methods to automatically recognize surface images.

Hinton *et al.* [11] proposed deep learning in 2006, and it is a new discipline of machine learning. There have been some studies on using deep learning to predict roughness. Liu *et al.* [12] proposed an on-machine surface defect detection method based on light scattering and deep learning. The scattering data was fed into a trained deep learning model to detect defects. Experimental results showed that the trained CNN model could identify any scattered signal associated with the surface within the range of simulation parameters. Rifai *et al*. [13] proposed to use a convolutional neural network to evaluate surface roughness directly from surface images, and they chose and analyzed five loss functions before concluding that the model with the MAPE loss function had the best accuracy. The model can be used to predict the surface roughness of typical machining operations such as outer diameter turning, groove milling and side milling under different cutting conditions. Saeedi *et al*. [14] used a convolutional neural network as a regression to obtain steel surface roughness. In the case of 14,000 images in the data set, the average percentage error of roughness prediction was 7.32%. Yeganefar *et al*. [15] compared the performance of regression analysis, a support vector machine, an artificial neural network and a multi-objective genetic algorithm in predicting and optimizing aluminum alloy cutting force and surface roughness. The study showed that the prediction performance of the neural network model was superior to that of other methods when the quantity of samples was sufficient. Although the roughness prediction method based on neural network mentioned above does not require artificial evaluation indexes, it requires a large number of samples for training. The model's generalization performance will be inadequate if the training samples are insufficient. Machining procedures like as turning, milling, and grinding, on the other hand, are time-consuming, labor-intensive, and lack controllability. It is difficult to establish a roughness sample database simply through experiments.

To overcome the difficulty of obtaining samples of various roughness levels and compensate for the absence of training sample data, simulation can be used to generate a large number of surface images with roughness labels. Liu *et al.* [16] proposed a light scattering method to identify classes of structured surface topographies and estimate their main geometric properties.

Metrol. Meas. Syst., Vol. 30 (2023), No. 1, pp. 117–138
DOI: 10.24425/mms.2023.144401

Experimental results showed that the proposed method could reconstruct the surface topography from the light scattering signal. Zhang *et al*. [17] obtained simulation data by constructing an optical simulation model for surface imaging. The simulation system consisted of a red and green light source system, an imaging system and a grinded workpiece. The imaging system used an Object for Video Disks lens. In the article, the specific imaging process was as follows: a customized red and green light source shone onto the surface of the workpiece, the light was then reflected through the surface of the workpiece into the lens, which next captured the virtual image formed by the red and green light source on the surface of the workpiece. They discovered through experiments that when the grinding surface roughness rises, the red and green aliasing effect of the actual images and the simulated images increased as well, and an aliasing area index was created based on color information. But the simulated image and the measured image belong to two different domains. To solve the problem of data mismatch between different domains, transfer learning is used to apply the knowledge learned in one domain or task to different but related domains to improve the accuracy of prediction. This method, however, necessitates the use of a dedicated red and green light source, which is not ideal for online visual inspection in a complicated light source environment in industrial production and is only suitable for grinded surfaces with a wide light diffusing surface. In the case of the milling surface, since the microscopic peaks and valleys of the surface are relatively rare compared to the grinding surface, the diffuse reflection surface of the point light source is small, so the red and green aliasing effect of the red and green light sources on the milled surface with different roughness is not very different. However, with the increase of the roughness of the milling surface, the texture spacing increases regularly, and the texture outline becomes more and more obvious. This feature is also reflected in milling optical simulation images. Therefore, these features can be matched according to actual milling images and optical simulation images through transfer learning. For the reasons stated above, a deep transfer learning Deep CORAL was utilized in our study to match actual photos to optical simulation images utilizing texture features. A measurement approach to milling surface roughness level based on Deep learning combined with simulation data was proposed based on the texture matching experiment. This method not only makes up for the problem of insufficient data samples, but also has good robustness to brightness.

2. Texture matching model and prediction model

2.1. Edge extraction texture and matching process

The spacing of milling texture grows regularly as roughness increases in actual milling images, and texture contour becomes more and more evident. The milling optical simulation images reflect this aspect as well. Due to the difference between the source domain of optical simulation images and actual images, however, the model trained directly using simulation data has a poor generalization ability to predict actual data in the target domain. Transfer learning can apply the knowledge learned in a certain domain or task to different but related domains, and can simultaneously learn the common features of both simulation domain and actual domain, so as to improve the prediction accuracy of target domain. Therefore, this paper uses the Laplace algorithm [18] for edge extraction to extract texture from actual and optical simulation images. When a limited number of actual texture images and a large number of optical simulation texture images are available, a small number of actual texture images and a large number of optical simulation texture images can be used in a Deep CORAL model as a mixed domain for training to learn the common features of the labeled mixed domain and the unlabeled actual

domain. The features from the same class will be more clustering, and finally achieve the matching accuracy of the real domain. Figure 1 shows the flow chart of texture level classification matching.

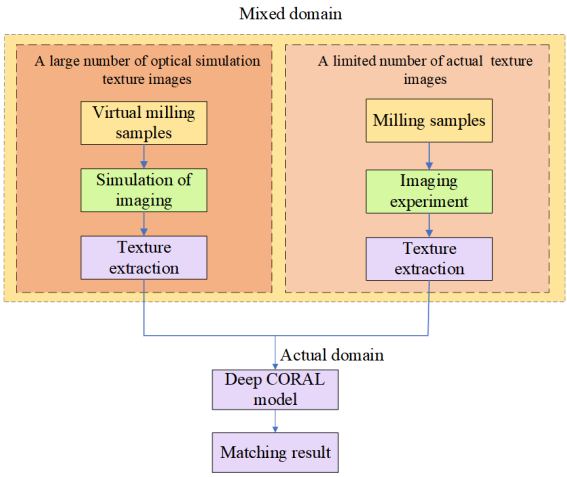

Fig. 1. Flow chart of texture level classification matching.

2.2. Deep CORAL model for texture-level classification matching

The Deep CORAL model combines feature extraction, feature transformation, and feature classification to uncover similar characteristics between the mixed domain and the actual domain, allowing for a significant reduction in the distance between the two domains. When there is only a small amount of real data, these shared features can be transferred from the simulation data to improve the performance of the model in the real domain and achieve end-to-end milling texture-level classification matching.

2.2.1. Objective function of the Deep CORAL model

The deep CORAL model is the addition of a CORAL [19] algorithm to the deep neural network AlexNet [20]. In the task of texture-level classification and matching, the CORAL algorithm is extended and integrated into the last connection layer of AlexNet, so that the CORAL loss is directly brought into the deep network. CORAL is a simple unsupervised adaptive method that minimizes the domain difference by adjusting the second-order statistics of data distribution of the mixed domain and the actual domain, and optimizes the CORAL loss to the minimum for the actual and mixed domains. The CORAL loss function L_{CORAL}, which describes the CORAL loss function of a single feature layer between the two domains, is defined as the second-order statistical feature distance between the mixed domain features and the actual domain features, and can be expressed as follows:

$$L_{\mathrm{CORAL}} = \frac{1}{4d^2} \|C_A - C_B\|_F^2 \tag{1}$$

where $\|\cdot\|_F$ represents the Frobenius norm of the square matrix. If it is assumed that the mixed domain training sample $D_A = \{x_i\}$, $x \in R^d$, label $L_S = \{y_i\}$, there are n_A data, the dimension is d; unlabeled real domain data $D_B = \{u_i\}$, $u \in R^d$, there are n_B data, dimension d; x and u here are both d dimensions of the deep activation $\varphi(I)$ to be learnt from the input image I, Then

Metrol. Meas. Syst., Vol. 30 (2023), No. 1, pp. 117–138
DOI: 10.24425/mms.2023.144401

covariance matrices C_A and C_B of mixed domain data and actual domain data can be calculated by formula (2) and formula (3):

$$C_A = \frac{1}{n_A - 1}\left(D_A^B D_A - \frac{1}{n_A}(\mathbf{1}^B D_A)^2(\mathbf{1}^B D_A)\right) \tag{2}$$

$$C_B = \frac{1}{n_B - 1}\left(D_B^B D_B - \frac{1}{n_B}(\mathbf{1}^B D_B)^2(\mathbf{1}^B D_B\right), \tag{3}$$

where $\mathbf{1}$ is the column vector where all elements are equal to 1.

The objective function of Deep CORAL includes both texture classification loss and CORAL loss, which can be expressed as follows:

$$L = L_{\text{CLASS}} + \lambda L_{\text{CORAL}}, \tag{4}$$

where λ is a parameter used to weigh the classification accuracy in the mixed domain and the adaptive performance in the actual domain, and L_{CLASS} is the classification loss in the mixed domain, which is calculated according to the following formula:

$$L_{\text{CLASS}} = -\sum_{c=1}^{c}\frac{1}{n_c}\sum_{i=1}^{n_c} y^i \log p^i \tag{5}$$

where C represents the number of label categories, n_c is the number of samples in the c-th category of the mixed domain, and $y_i(p_i)$ is the true label (predicted label) of the i-th mixed-domain sample.

CORAL loss and texture classification loss play corresponding roles in the process of training the model, and they reach a balance at the end of training. The ultimate goal is to optimize the texture classification loss and CORAL loss to the minimum, so that the mixed domain classification is more accurate and the output of the actual domain is more comparable to the distribution of the mixed domain.

2.2.2. Structure of the deep CORAL model

The structure of Deep CORAL is shown in Fig. 2. It can be seen from the figure that the model applies the CORAL algorithm to the last layer of AlexNet (Fc8), and the structure of the first 7

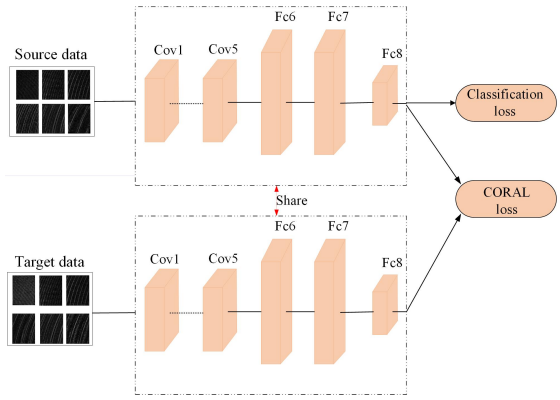

Fig. 2. Structure of Deep CORAL.

layers is exactly the same as that of ordinary AlexNet. The network combines the data from the mixed domain and the data from the actual domain to train itself. To acquire classification loss, the mixed domain data output is supervised and trained using the mixed domain label. However, as there is no labeled data for supervised training in the output of actual domain data, it is necessary to adapt to the mixed domain data and calculate CORAL loss.

2.2.3. Training process of Deep CORAL model

It is difficult to get a significant number of milling workpiece images in the field of machining, and a neural network recognition model with strong generalization ability cannot be obtained with only a small amount of data. Therefore, the Deep CORAL model first uses the AlexNet model integrating a CORAL algorithm to train the ImageNet of tens of millions of image data to get the pre-training model. Second, it preprocesses the labeled mixed domain data and the unlabeled actual domain data, and then inputs the set roughness level image data into the pre-trained AlexNet network for fine-tuning. After the convolution of the AlexNet network, the maximum Pooling, LRN, dropout and other operations, the joint distribution function L of classification loss, coral loss and deep coral is calculated, and then the parameters of each layer are adjusted through backpropagation. Finally, when the loss entropy tends to be stable, converges or reaches the preset training times, the Deep CORAL model of milling texture level classification matching can be obtained after the training. The main parameters and training process of Deep CORAL model are shown in Table 1 and Fig. 3, where "batch size" is the number of samples to train the model once, an "epoch" is the number of iterations supposed to train all the training images through the model

Table 1. Main parameters of the Deep CORAL model.

Batch size	Epoch	Dropout	Learning rate
32	50	0.5	0.0001

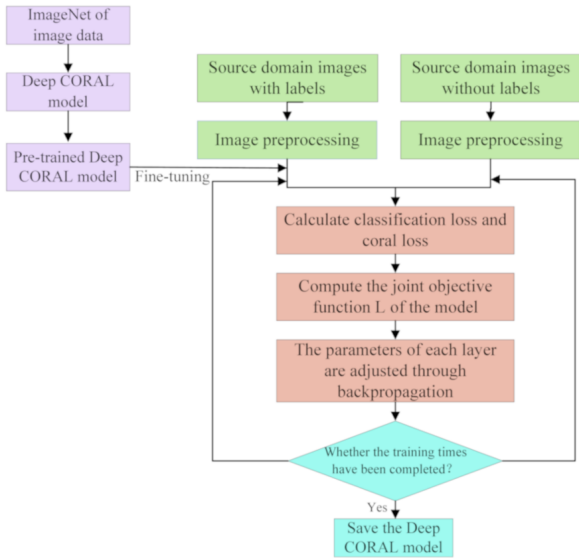

Fig. 3. Diagram of the Deep CORAL model processing.

Metrol. Meas. Syst., Vol. 30 (2023), No. 1, pp. 117–138
DOI: 10.24425/mms.2023.144401

once, "dropout" reduces the problem of model overfitting and the "learning rate" characterizes the rate at which information accumulates over time in a neural network.

2.3. Xception model for roughness level prediction

The texture information of each type of roughness image in the training set such as the texture of the milling surface, the width of the texture, and the radian of the texture is thought to be highly important in the Xception model. The neural network will extract and use this data during model training to improve the model's accuracy and effectiveness [21]. Therefore, this paper first realizes the matching between the simulated texture images and the actual texture images, and then inputs the simulation images and the actual images into the Xception model to predict the roughness.

The following is the training procedure for the Xception model based on roughness level prediction: First, the data flow diagram of CNN model is initialized, including creating network structure and initialization parameters, the data set divided according to roughness level into the Xception model for training is imported. Second, error is calculated using the loss function, and then the parameters of each layer are modified using back propagation. After that, new network parameters are output and saved, including the iteration number, validation set accuracy and loss entropy value. Finally, the training is completed when loss entropy tends to be stable, converges or reaches the preset training times. Parameter values involved in the training process of the Xception model and the training process are shown in Table 2 and Fig. 4.

Table 2. Parameter values involved in the training process of the Xception model.

Batch size	Epoch	Dropout	Learning rate
32	100	0.5	0.0001

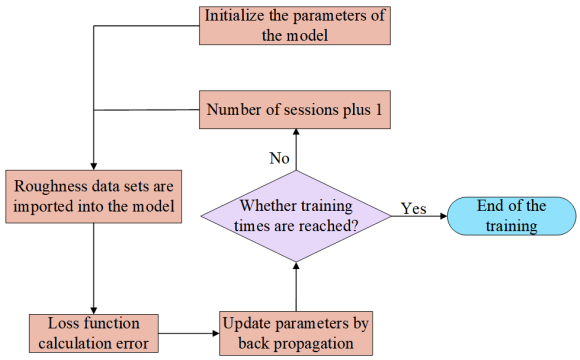

Fig. 4. Process of Xception model training.

3. Experiment

The experiments include milling sample preparation, image acquisition, texture level classification matching experiment and roughness classification prediction experiment. The experimental flow chart is shown in Fig. 5.

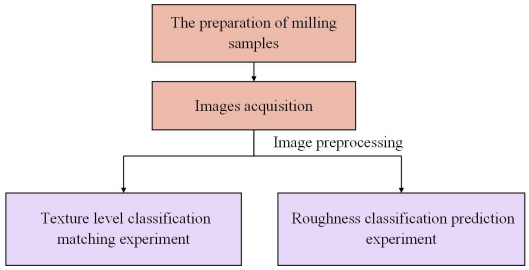

Fig. 5. Experimental flow chart.

3.1. Sample preparation

The preparation of milling samples includes the preparation of actual samples and simulation samples.

In recent years, with the development of artificial intelligence, it has been more and more widely used in the field of measurement [22]. In order to improve the efficiency and quality of measurement, more and more scholars have searched to show the relationship between morphological features and parameters [23, 24], and even proposed new parameters. In surface roughness machining processes, whether the machined surface roughness profile meets the requirements should be quantified by a series of evaluation parameters. ISO 21920-2-2021 (Geometrical product specifications (GPS) – Surface texture: Profile – Part 2: Terms, definitions and surface texture parameters) provides definitions and methods for assessing surface roughness parameters by the profile method. The main evaluation parameters of the roughness profile are the sampling length *Lr*, the maximum profile peak height *Rp*, and the maximum profile height *Rz*. Besides, there are the arithmetic average roughness value *Ra*, etc. Among the evaluation parameters, the concept of *Ra* is intuitive and provides the most comprehensive characterization of the small peaks and valleys of the workpiece surface profile. Therefore, *Ra* is the most commonly used evaluation parameter in industrial production. *Ra* was also used as the roughness evaluation parameter in this paper.

To obtain 24 milled workpieces with uniform surface finish, a Lunan XHS7145 CNC machine and the FANUC Series Oi Mate-MD operating system with a TAP400R100-32-6T vertical disc milling cutter was used to mill a series of 45# steel blocks with an area of 40×60 mm^2 under the parameters of cutting depth of 0.05 mm, spindle speed of 700 r/min and disc tool feed speed of 200–2200 mm/min. The surface roughness of 24 milling surfaces was sampled and measured at 6 places using a TR210 stylus roughness measurement instrument with a resolution of 0.001 µm and a standard sensor probe. The workpiece's surface roughness was calculated using the average of the 6 measurements. The surface roughness measurement results of the milling workpiece are shown in Table 3.

In the process of measuring roughness, the stylus roughness measuring instrument can get different roughness values at different positions on the surface of a milling sample block as they can fluctuate. Therefore, the roughness can be divided into several roughness grades. According to the measurement results, the roughness grades were classified into 6 categories: [0.4–0.7), [0.7–1), [1–1.4), [1.4–1.8), [1.8–2.2), [2.2–2.6).

The simulation sample object created through simulation milling is referred to as a simulation sample. The specific process is as follows: first, according to the cutting behavior of the milling cutter when cutting the workpiece, combined with the effective cutting time of each cutter tooth, the contact area of the workpiece is determined [25]. Second, process parameters are entered

Metrol. Meas. Syst., Vol. 30 (2023), No. 1, pp. 117–138
DOI: 10.24425/mms.2023.144401

Table 3. Surface roughness measurement results for each milled workpiece (*Ra*, unit: µm).

NO	Type	First	Second	Third	Forth	Fifth	Sixth	Avg
1	1	0.659	0.600	0.678	0.635	0.671	0.625	0.645
2	1	0.682	0.583	0.485	0.434	0.399	0.600	0.531
3	1	0.452	0.463	0.447	0.639	0.492	0.480	0.496
4	1	0.550	0.673	0.59	0.604	0.549	0.622	0.598
5	2	0.638	0.651	0.682	0.767	0.588	0.892	0.703
6	2	1.209	1.036	0.633	1.051	1.191	0.762	0.980
7	2	1.106	1.097	0.880	0.817	1.155	0.916	0.995
8	2	0.732	0.619	0.799	0.687	0.637	0.762	0.706
9	3	1.202	1.128	1.244	1.258	1.300	1.042	1.196
10	3	0.893	1.003	1.153	1.141	1.265	1.227	1.114
11	3	1.671	1.240	1.274	1.206	1.247	1.385	1.337
12	3	1.292	1.512	1.329	1.383	1.491	1.365	1.395
13	4	1.544	1.346	1.582	1.455	1.556	1.250	1.456
14	4	1.780	1.744	1.696	1.651	1.558	1.492	1.654
15	4	1.763	1.752	1.751	1.909	1.693	1.862	1.788
16	4	1.831	1.769	1.734	1.591	1.724	1.809	1.743
17	5	1.942	1.831	1.716	1.793	1.760	1.769	1.802
18	5	2.097	1.848	1.700	1.750	1.830	1.677	1.817
19	5	1.779	1.712	1.825	1.999	1.833	1.671	1.803
20	5	2.378	2.128	2.133	2.066	2.110	2.334	2.192
21	6	2.239	2.298	2.147	2.408	2.330	2.412	2.306
22	6	2.450	2.785	2.473	2.704	2.416	2.390	2.536
23	6	2.691	2.541	2.675	2.554	2.689	2.443	2.599
24	6	2.613	2.539	2.447	2.612	2.430	2.512	2.526

into MATLAB, and the height Z-value of each coordinate point (x, y) on the XY plane in the Z-direction is recorded based on a z-Map model [26, 27]. In this way, the simulated surface topography of the discrete representation of the virtual workpiece is obtained (as shown in Fig. 6a), with roughness ranging from 0.3 µm to 2.6 µm. Finally, 3D modeling software SolidWorks is used to create virtual sample entities (as shown in the Fig. 6b).

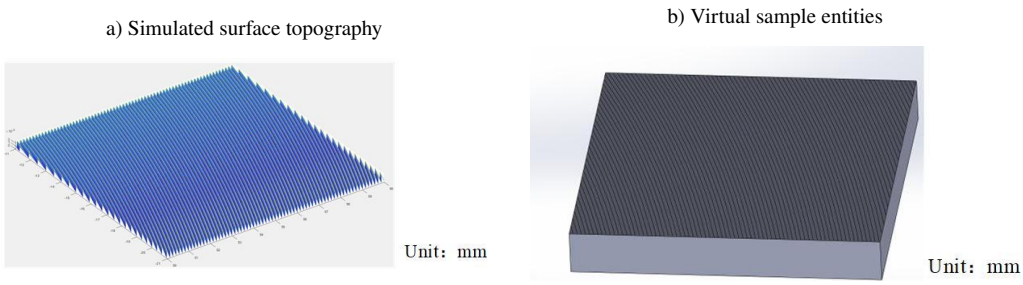

Fig. 6. Virtual sample.

3.2. Image acquisition

In order to obtain the image information of roughness of the actual milling sample, the milling workpiece is placed flat on the precision optical platform and parallel to the platform; the optical axis of the camera is perpendicular to the measured surface of the sample. During the experiment, the relative positions of the camera, light source and sample remain unchanged.

Figure 7a depicts the experimental apparatus, which is made up mostly of the following components: 1) a Basler color CCD camera equipped with a VS-2514H1 industrial camera lens; 2) an OPT-LI14030 white strip light source; 3) an OPT -DPA1024E-4 light source controller; 4) a computer; 5) the pylon Viewer program controls the color CCD camera which takes and stores photographs of the milled workpiece. The obtained images of the milled workpieces are shown in Fig. 7b.

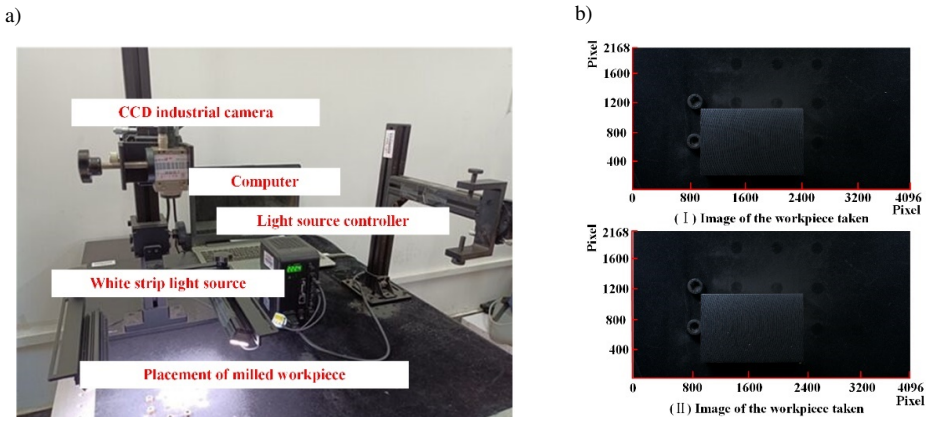

Fig. 7. Experimental apparatus and milled workpieces. a) Experimental apparatus. b) Images of the workpieces taken by the CCD camera.

Due to the too large size of the original image, the workpiece area in each milling workpiece image is divided into 6 non-overlapping areas with a size of 100×100 pixels, and 6 types of data sets are obtained after cropping according to the area. The set contains 72 workpiece images, and a roughness sample database is established for the texture level classification matching and roughness classification prediction experiments. The milled workpiece after cutting is shown in Fig. 8.

To obtain the roughness image information of virtual milling samples, the virtual three-dimensional sample was imported into the optical simulation TracePro software. The simulation model has three components: a white light source system, an imaging system and the simulation workpiece. The OPT-LI14030 white bar light is used in the acquisition of the actual milled sample images, so that a white light source is included in the simulation model. In an imaging system, there are three key physical quantities i.e., the object distance, image distance and focal length. The distance between the object and the center of the lens becomes the object distance. The distance between the image and the center of the lens is called the image distance. The point at which parallel light is focused after passing through the lens is called the focal point, and the distance between the focal point and the center of the lens is called the focal length. The three satisfy the following relationship:

$$\frac{1}{u} + \frac{1}{v} = \frac{1}{f}, \tag{6}$$

Metrol. Meas. Syst., Vol. 30 (2023), No. 1, pp. 117–138
DOI: 10.24425/mms.2023.144401

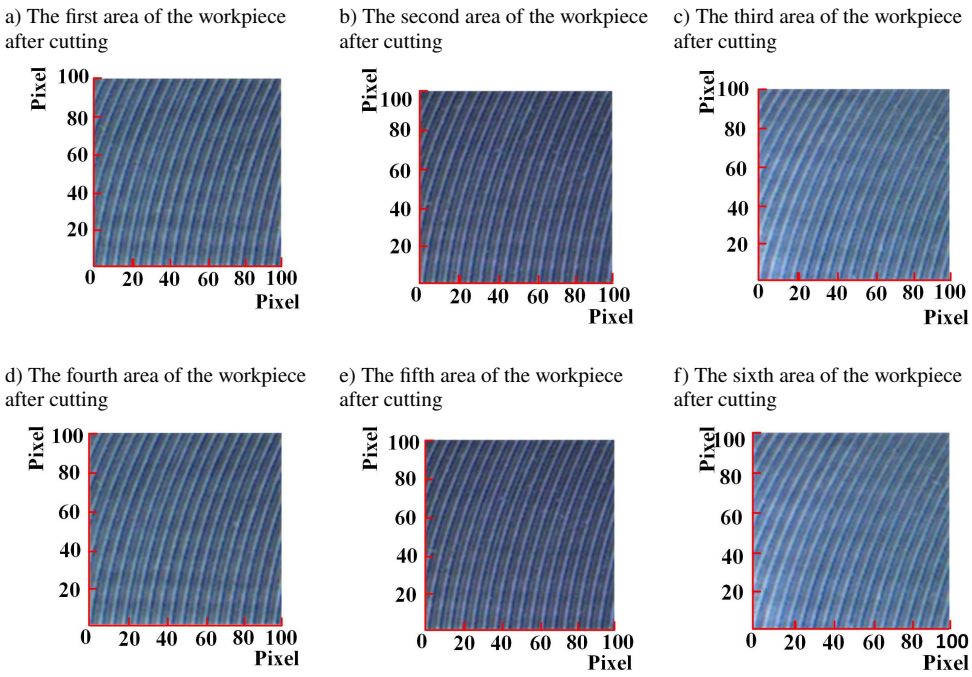

Fig. 8. Milled workpiece after cutting.

where u is the object distance, v is the image distance and f is the focal length. This article uses a simulation of an industrial camera in which the simulated lens is a compound lens invented by John Henry Dallmeyer so that the object and image distances need to be adjusted to satisfy the premise of equation 1, so that the imaging law is $u > 2$, $f < v < 2f$ to obtain an image in the imaging plane. Finally, the milled simulation workpiece is generated using the 3D modeling software SolidWorks. The specific working process of the simulation model is as follows: the white light source shines on the surface of the simulation workpiece, and then reflects into the simulation lens. Finally, the reflected image of the simulation workpiece is generated through the lens. Figure 9a depicts the optical simulation model, while Figure 9b depicts the optical simulation images.

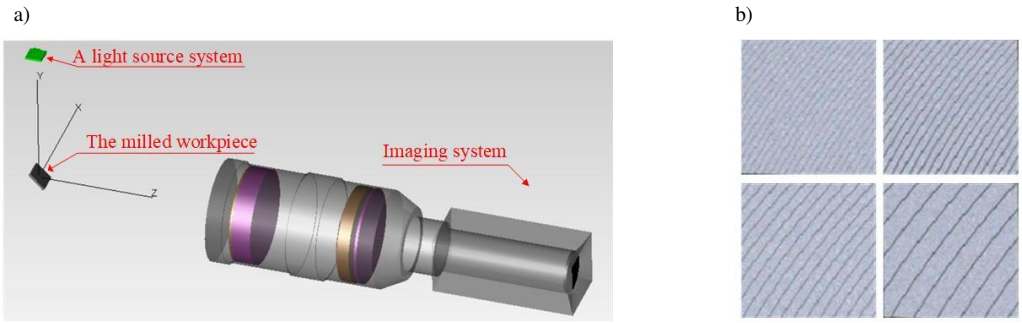

Fig. 9. The optical simulation model and the optical simulation images. a) Optical simulation model. b) Optical simulation images.

3.3. Texture level classification matching experiment

This paper uses the Laplace algorithm for edge extraction to extract texture from actual and optical simulation images. Figure 10 shows an actual texture image and an optical simulation texture image of the same level.

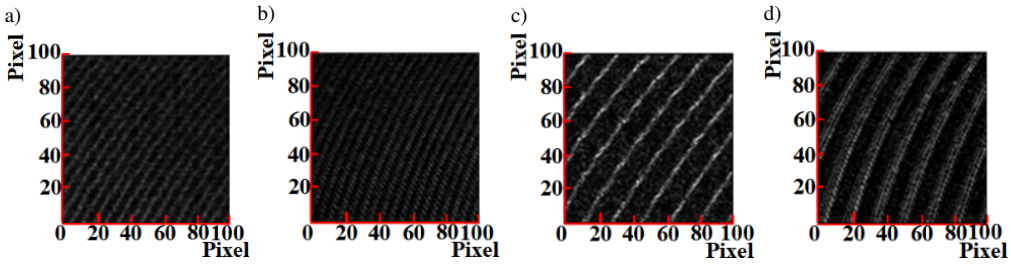

Fig. 10. Actual texture images and optical simulation texture images of the same level.

Transfer learning can transfer the knowledge learned in the simulation domain to the actual domain and learn the common features of the two domains, so as to improve the prediction accuracy of the target domain. However, due to the difference in data distribution between the simulation domain and the actual domain, if the simulation data is directly used to predict the actual data, the trained model may be more suitable for the simulation domain and have a poor generalization ability in the actual domain [13]. As a result, the following two comparison studies are designed in this work to validate the degree of matching between the optical simulation texture images and the actual texture images:

Experiment A: In the prepared roughness sample database, 50 images of each class were randomly selected as training sets and textures were extracted. 50 images were randomly selected from the remaining database images as the test set.

Experiment B: 40 actual texture images in each category of the experiment A were replaced with optical simulation texture images, and 10 actual texture images were retained. The test set was the same as in Experiment A. The specific experimental steps are shown in Fig. 11.

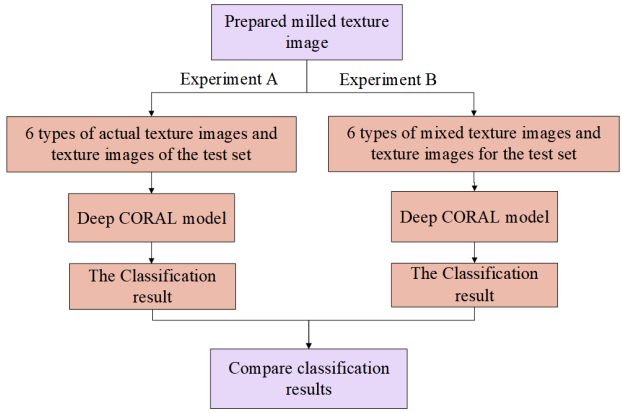

Fig. 11. Specific experimental steps.

Metrol. Meas. Syst., Vol. 30 (2023), No. 1, pp. 117–138
DOI: 10.24425/mms.2023.144401

3.4. Roughness classification and prediction experiment

Deep learning has certain requirements on the data volume of the data set and it is necessary to expand the surface images of 6 types of milling workpieces (including actual images and optical simulation images). The image is preprocessed by flipping, rotating, saturation adjustment, contrast adjustment, hue adjustment, and shifting to enhance the original dataset.

The influence of adding simulation data on classification prediction accuracy is compared in the following three experiments:

Experiment 1: The training set consisted of 6 types of surface images of milling workpiece after data enhancement, all of which were actually taken.

Experiment 2: Optical simulation images were added to the training set on the basis of Experiment 1. After data enhancement, the ratio of each type of actual image to optical simulation image was 2:1.

Experiment 3: On the basis of Experiment 2, the ratio of each type of actual image and optical simulation image was adjusted to 1:2.

The three experiments were conducted using the same test set. The specific experimental steps are shown in Fig. 12.

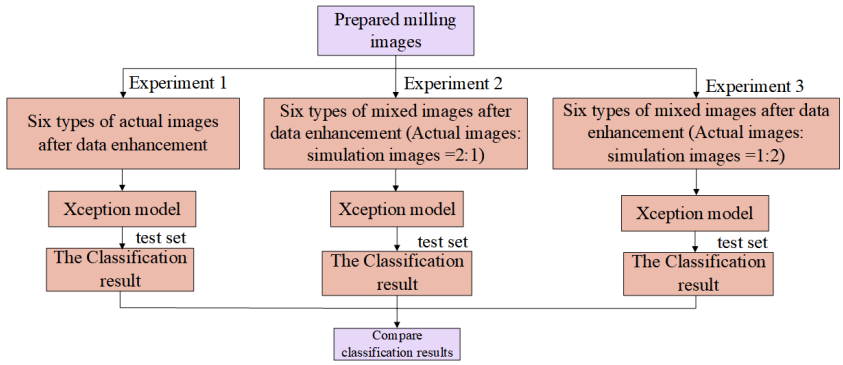

Fig. 12. Specific experimental steps.

Table 4 shows the classification and quantitative statistics of samples after data enhancement in Experiments 1, 2 and 3.

Table 4. Number of roughness images for each grade after data enhancement in Experiment 1, 2 and 3.

Roughness (unit: um)	0.4–0.7	0.7–1.0	1.0–1.4	1.4–1.8	1.8–2.2	2.2–2.6	**In total**
Number of data sets (unit: pieces)	200	200	200	200	200	200	1200
	300	300	300	300	300	300	1800

In the roughness classification prediction Xception model, the sample set can be divided into a training set and a validation set. To balance training and validation in this experiment, the ratio of training and validation sets for each class of roughness images after data enhancement in Experiments 1, 2 and 3 is set to 8:2.

4. Experimental results

4.1. Experimental results of texture level classification matching

The fluctuation of the loss function and classification accuracy with epoch of the Deep CORAL model is depicted in the following figure based on experimental findings.

During the training of the Deep CORAL model, Epoch was chosen to be 50. As can be seen from Figure 13, the loss value of both experiment A and experiment B basically reached stability after Epoch=40, while the recognition accuracy also fluctuated within a small range, indicating that the model already had effective classification capability. As can be seen in Figure 13, after Epoch=40, the cross-domain recognition accuracy of both experiment A and experiment Bb was about 90%, which indicated that the recognition model based on deep transfer learning extracted the common features of the mixed texture images in the source domain and the actual texture images in the target domain, and further reduced the difference of feature metrics between the simulated and actual samples by learning the nonlinear transformation of the second-order statistics of the aligned source and target domain data distributions, and achieved the matching of the optical simulated texture images with the actual texture images.

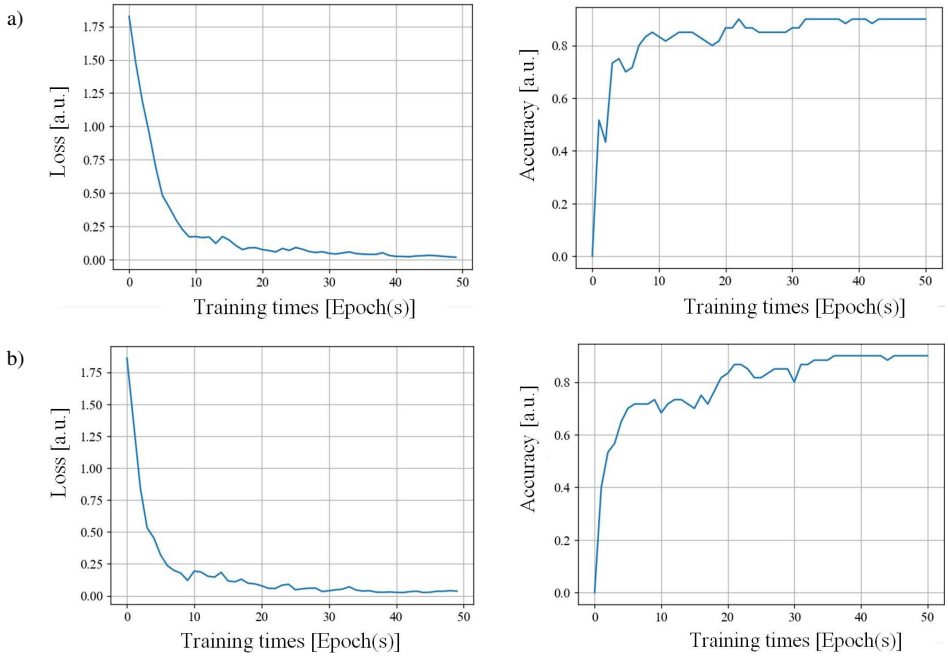

Fig. 13. Loss function and classification accuracy with different epochs of the Deep CORAL model.

4.2. Experimental results of roughness classification prediction

Using Tensorboard [28], a visualization tool in Tensorflow [29], the training loss curve and the accuracy curve of the Xception model are shown below, including the training and validation sets. The test sets of Experiments 1, 2 and 3 are all 111 images that are not involved in the training of the model.

Metrol. Meas. Syst., Vol. 30 (2023), No. 1, pp. 117–138
DOI: 10.24425/mms.2023.144401

4.2.1. The classification result of Experiment 1

Figure 14 shows that the overall loss curve of the roughness classification model converges as the number of Epoch increases, and after the Epoch = 50, despite minor fluctuations, the loss value converges to within 0.05, and the model validation set accuracy becomes stable, suggesting that the model has learned the data features from the roughness dataset, and it has achieved the expected results. When the test set was tested, the accuracy reached 86.48%.

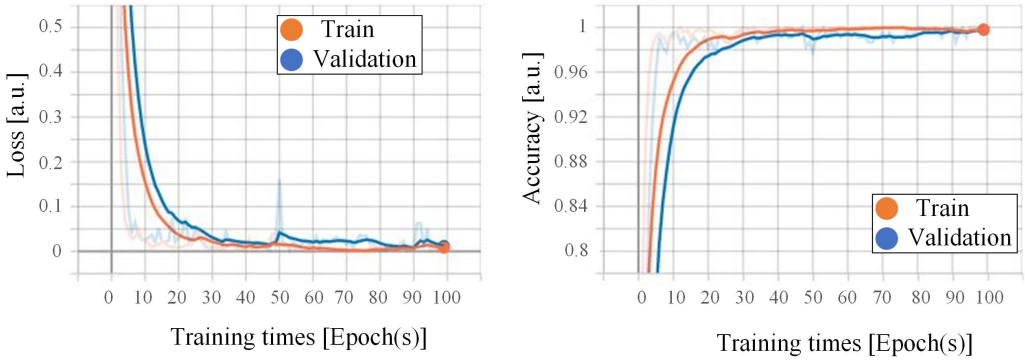

Fig. 14. Training loss curve and accuracy curve of the Experiment 1.

4.2.2. The classification result of Experiment 2

Similarly, it can be seen from Fig. 15 that the model loss values converge to 0.04 after Epoch = 43, and the model has learned the data features from the roughness dataset. After Epoch=43, the accuracy of the validation set remains at 99%, also proving the valid classification capability of the model. When tested in the test set, the accuracy reaches 92.79%.

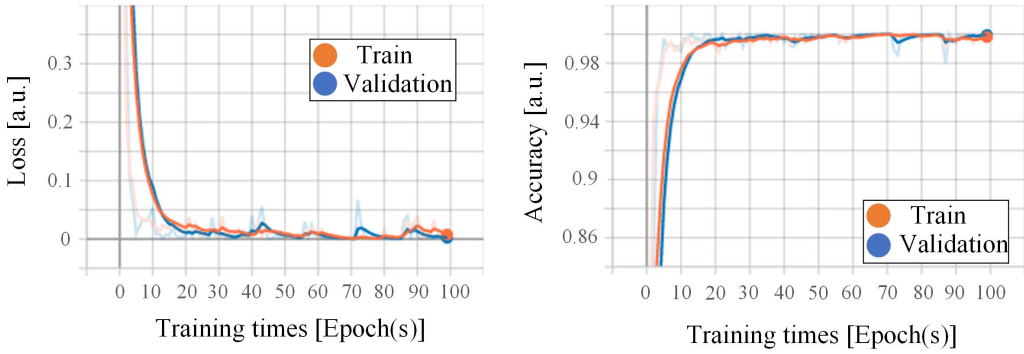

Fig. 15. Training loss curve and accuracy curve of the Experiment 2.

4.2.3. The classification result of Experiment 3

Similarly, when the test set test was performed, the accuracy reached 92.79% (Fig. 16).

In order to study the effect of simulation data on classification prediction accuracy, three experiments were done for this study. The training set of Experiment 1 consisted of all the actual images taken, the training set of Experiment 2 were the simulation images added on the basis of

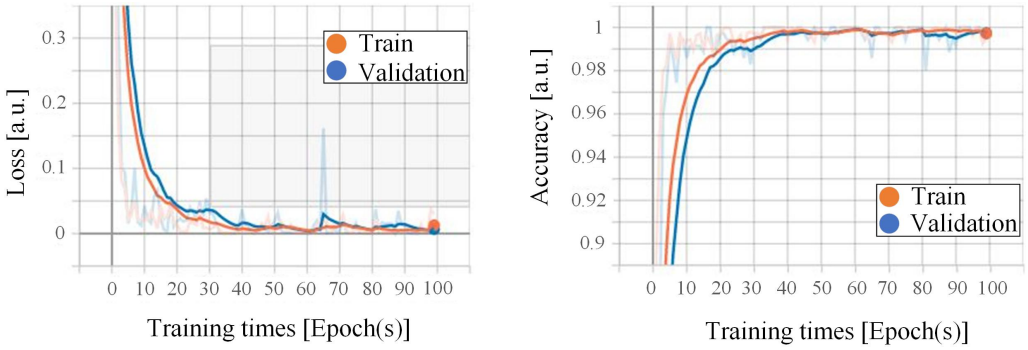

Fig. 16. Training loss curve and accuracy curve of the Experiment 3.

Experiment 1, and Experiment 3 was to adjust the number of actual images and simulation images in Experiment 2, so that the number of actual images was less than the number of simulation images. As can be seen from the results of Experiments 1 and 2, the accuracy rate increased from 86.48% to 92.79%. In Experiment 3, with less data from the actual milled pictures, the model accuracy was also 92.79%. This is because, in the Xception model, it is assumed that the texture information of each grade of roughness picture in the training set, such as the texture of the milling surface, the width of the texture, the curvature of the texture, etc. is very significant. The information is extracted and used by the neural network in the model training, making the model more accurate and effective [16]. Therefore, in this paper, the simulated texture was matched with the actual texture first, and then the simulated images and the actual images were input into the Xception model to predict the roughness.

5. Discussion

In the Xception model based on roughness level prediction, the convolutional and pooling layers of the convolutional neural network can respond to the translational invariance of input features, that is, they can recognize similar features located at different locations in space and can extract high and low frequency features of the image from the input two-dimensional image pixels, such as the underlying detail features of the image like texture and color, and extract general and combinatorial features in the deeper structure. In this paper, the brightness, color and texture of the Xception model training set were changed respectively to study which factor has the greatest influence on the Xception model. For the change of brightness and color in the training set, it was changed by computer programming, while the test set was unchanged. The influence of color and brightness on the Xception model was studied through the prediction results of the test set.

5.1. Brightness and color

Experiment 3 in Section 4.2 investigates the impact of brightness and color on the Xception model by adjusting the brightness and color of the training data. The basic principle of the program for changing brightness is to adjust the values of the three color components R, G and B in the RGB [30] space. According to the principle of the RGB color, to adjust the brightness of a color, we can add the same amount of adjustment n to the three color components of red, green and blue, and n is an integer between $[-255, 255]$. When the amount of adjustment n is added,

Metrol. Meas. Syst., Vol. 30 (2023), No. 1, pp. 117–138
DOI: 10.24425/mms.2023.144401

the image after adjusting the brightness can be obtained. To change the color of the training set, it is necessary to change the value of H in HSV [31]. Through different values of H, the picture can be converted into different colors. The specific steps are: (1) Get the RGB value of each pixel of the image; (2) Convert the RGB value to HSV value; (3) Modify the H in the HSV color value; (4) Convert the HSV value back to RGB value; (5) Output the image.

A comparison of the training set after changing the brightness and color is shown in Fig. 17. After changing the brightness and color consecutively, the Xception model training loss curve and accuracy curve are shown in Figs. 18 and 19. When testing on the test set, the accuracy rates were 92.79% and 88.28% respectively. The experimental results revealed that the Xception model has better robustness to brightness and color, proving the conclusion in the literature that the Xception model of deep convolutional neural networks is robust to light source environment [16], but the Xception model is more sensitive to color information than brightness.

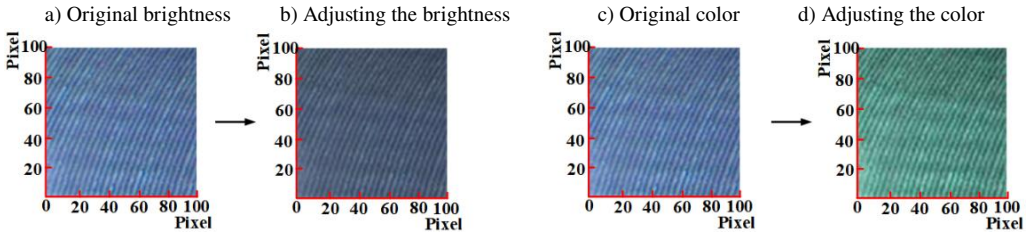

Fig. 17. Comparison of the training set after changing the brightness and color.

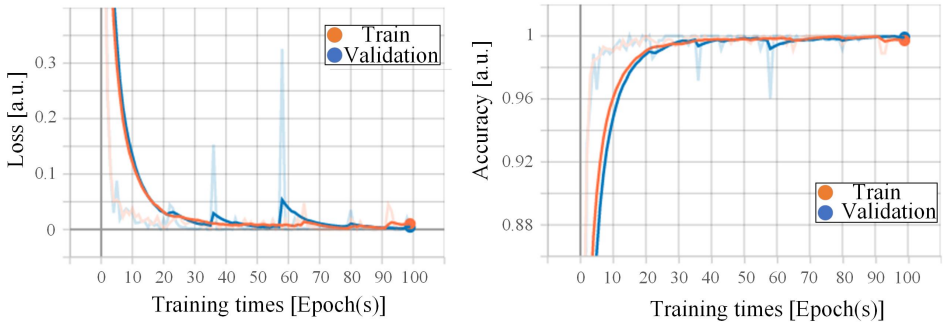

Fig. 18. Xception model training loss curve and accuracy curve after changing the brightness.

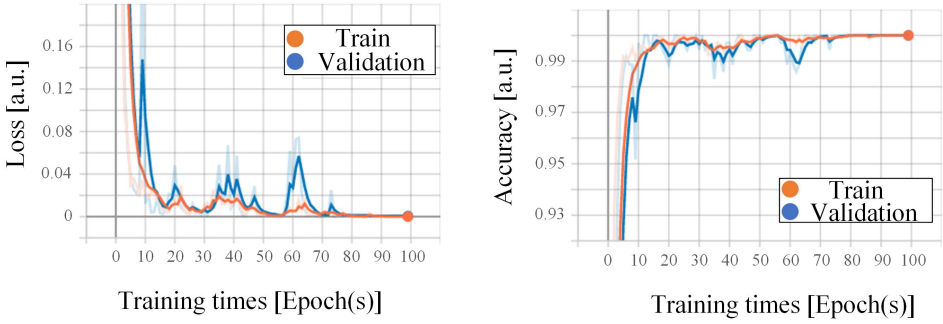

Fig. 19. Xception model training loss curve and accuracy curve after changing the color.

5.2. Texture

With the increase of feed rate, the milling texture spacing shows a regular increase and the texture profile becomes increasingly visible. Therefore, among the 6 types of roughness grades, the texture characteristics of the milled surface are significantly different. In order to study the effect of texture on the prediction accuracy of the Xception model, the process parameters were changed to generate new 3D milling virtual samples under the premise that the roughness range was consistent, so that the textures of each class were different from the previous ones. Then the images were generated by an optical imaging system. Finally, the newly generated optical simulation image was imported into the Xception model for training and the effect of texture on the Xception model was studied through the test results. Fig. 20a shows the original optical simulation images and Fig. 20b shows the newly generated optical simulation images. The Xception model training loss function curve and the accuracy curve are shown in Fig. 21. The accuracy rate is 76.57% in test set testing.

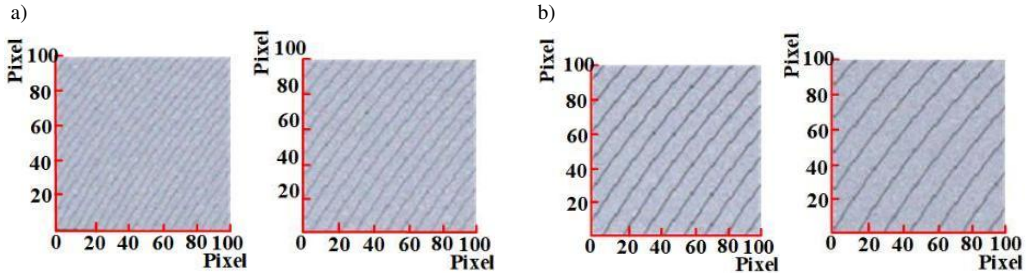

(I) The original optical simulation image 1. (II) The original optical simulation image 2. (III) The newly generated optical simulation image 1. (IV) The newly generated optical simulation image 2.

Fig. 20. Original optical simulation images and newly generated optical simulation images. a) Original optical simulation images. b) Newly generated optical simulation images.

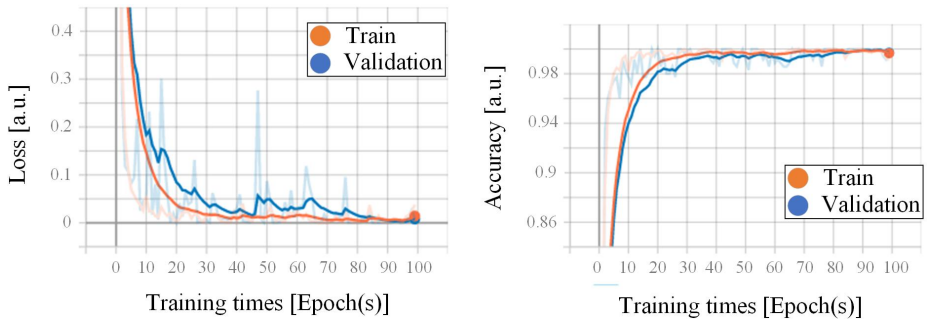

Fig. 21. Xception model training loss curve and accuracy curve after changing texture.

The texture information of each class of roughness photos in the training set is assumed to be extremely important, and this information will be extracted and used by the neural network in the model training, so the optical simulation images added in Experiments 2 and 3 in Section 4.2 of roughness classification prediction can enrich the dataset of milling images. However, after importing the newly generated optical simulation images into the model in the altered texture experiments in Section 4.2, there is some interference with the model extracted information,

Metrol. Meas. Syst., Vol. 30 (2023), No. 1, pp. 117–138
DOI: 10.24425/mms.2023.144401

reducing the accuracy rate, which is the reason for why the simulation texture matching with the actual texture is needed.

In conclusion, texture has the greatest influence on the prediction accuracy of the Xception model, followed by color and brightness, which has good robustness.

6. Conclusions

1. To solve the problem of different domains between simulation samples and actual samples, a transfer learning Deep CORAL model was adopted to conduct cross-domain matching between simulation samples and actual samples. The experimental results show that the optical simulation images and the actual images can achieve high texture matching degree, which lays a foundation for using the simulation images to extend the actual milled workpiece images.
2. To address the problem that deep neural networks require a sufficient number of training samples to have a good prediction performance, a deep learning prediction method for milling surface roughness grade combined with simulation data is proposed based on texture matching experiments. The data was expanded by adding optical simulation images to the original six grade roughness dataset, the Xception network model was used to classify and identify the roughness images, and the accuracy was increased from 86.48% to 92.79% compared with the model without the simulation data. The method proposed in this paper is able to build an advanced roughness classification prediction model with fewer actual images.
3. In this paper, the brightness, color and texture of the Xception model training set were changed consecutively to study which factor had the greatest influence on Xception model. The experimental results show that surface texture had the greatest impact on the model prediction accuracy, followed by color, and the robustness to brightness is the best, which provides technical support for online visual detection under different light sources in industrial production.

Acknowledgements

This work was supported by the National Natural Science Foundation of China (NSFC) (Grant No. 52065016) and Guangxi Graduate Student Innovation Project in 2021 (Grant No. YCSW2021204).

Appendix I. Nomenclature

Abbreviations	Definition
Fc	fully connected layer
Cov	convolution
LRN	Local Response Normalization

Symbol	Definition
L	joint distribution function
L_{CORAL}	CORAL loss function
n_A	amount of data
n_B	amount of data

Symbol	**Definition**
D_A	mixed domain training sample
D_B	unlabeled real domain data
C_A	covariance matrix of mixed domain data
C_B	covariance matrix of actual domain data
C	number of label categories
n_C	number of samples in the c-th category of the mixed domain
$y_i\,(p_i)$	true label (predicted label) of the i-th mixed-domain sample
λ	parameter used to weigh the classification accuracy
L_{CLASS}	classification loss in the mixed domain
d	dimension
CNN	Convolutional Neural Network
Ra	Roughness parameters
Parameter Name	**Setting**
Batch	32
Epoch	50
Dropout	0.5
Learning rate	0.0001

References

[1] Wen, L., Ye, X., & Gao, L. (2020). A new automatic machine learning based hyperparameter optimization for workpiece quality prediction. *Measurement and Control*, *53*(7-8), 1088–1098. https://doi.org/10.1177/0020294020932347

[2] Leelawattananon, T., Thowladda, W., & Chittayasothorn, S. (2015, August). Surface roughness measurement application using multi-frame techniques. *In 2015 International Conference on Computer Application Technologies* (pp. 86–91). IEEE. https://doi.org/10.1109/CCATS.2015.30

[3] Guo, R., & Tao, Z. (2011). Experimental investigation of a modified Beckmann–Kirchhoff scattering theory for the in-process optical measurement of surface quality. *Optik*, *122*(21), 1890–1894. https://doi.org/10.1016/j.ijleo.2010.11.019

[4] Murugarajan, A., & Samuel, G. L. (2011). Measurement, modeling and evaluation of surface parameter using capacitive-sensor-based measurement system. *Metrology and Measurement Systems*, *18*(3), 403–418. https://doi.org/10.2478/V10178-011-0007-9

[5] Hamed, A. M., El-Ghandoor, H., El-Diasty, F., & Saudy, M. (2004). Analysis of speckle images to assess surface roughness. *Optics & Laser Technology*, *36*(3), 249–253. https://doi.org/10.1016/j.optlastec. 2003.09.005

[6] Jeyapoovan, T., & Murugan, M. (2013). Surface roughness classification using image processing. *Measurement*, *46*(7), 2065–2072. https://doi.org/10.1016/j.measurement.2013.03.014

[7] Kamguem, R., Tahan, S. A., & Songmene, V. (2013). Evaluation of machined part surface roughness using image texture gradient factor. *International Journal of Precision Engineering and Manufacturing*, *14*(2), 183–190. https://doi.org/10.1007/s12541-013-0026-x

[8] Lu, E., Liu, J., Gao, R., Yi, H., Wang, W., & Suo, X. (2018). Designing indices to measure surface roughness based on the color distribution statistical matrix (CDSM). *Tribology International*, *122*, 96–107. https://doi.org/10.1016/j.triboint.2018.02.033

Metrol. Meas. Syst., Vol. 30 (2023), No. 1, pp. 117–138
DOI: 10.24425/mms.2023.144401

[9] Yi, H., Liu, J., Ao, P., Lu, E., & Zhang, H. (2016). Visual method for measuring the roughness of a grinding piece based on color indices. *Optics Express*, *24*(15), 17215–17233. https://doi.org/10.1364/OE.24.017215

[10] Huaian, Y., Xinjia, Z., Le, T., Yonglun, C., & Jie, Y. (2020). Measuring grinding surface roughness based on singular value entropy of quaternion. *Measurement Science and Technology*, *31*(11), 115006. https://doi.org/10.1088/1361-6501/ab9aa9

[11] Hinton, G. E., Osindero, S., & Teh, Y. W. (2006). A fast learning algorithm for deep belief nets. *Neural Computation*, *18*(7), 1527–1554. https://doi.org/10.1162/neco.2006.18.7.1527

[12] Liu, M., Cheung, C. F., Senin, N., Wang, S., Su, R., & Leach, R. (2020). On-machine surface defect detection using light scattering and deep learning. *JOSA A*, *37*(9), B53–B59. https://doi.org/10.1364/JOSAA.394102

[13] Rifai, A. P., Aoyama, H., Tho N. H., et al. (2020). Evaluation of turned and milled surfaces roughness using convolutional neural network. *J. Measurement*, *161*, 107860. https://doi.org/10.1016/j.measurement.2020.107860

[14] Saeedi, J., Dotta, M., Galli, A., Nasciuti, A., Maradia, U., Boccadoro, M., Gambardella, L. M. & Giusti, A. (2021). Measurement and inspection of electrical discharge machined steel surfaces using deep neural networks. *Machine Vision and Applications*, *32*(1), 1–15. https://doi.org/10.1007/s00138-020-01142-w

[15] Yeganefar, A., Niknam, S. A., & Asadi, R. (2019). The use of support vector machine, neural network, and regression analysis to predict and optimize surface roughness and cutting forces in milling. *The International Journal of Advanced Manufacturing Technology*, *105*(1), 951–965. https://doi.org/10.1007/s00170-019-04227-7

[16] Liu, M., Senin, N., Su, R., & Leach, R. (2020, April). Cascaded machine learning model for reconstruction of surface topography from light scattering. In *Optics and Photonics for Advanced Dimensional Metrology* (Vol. 11352, pp. 174–182). SPIE. https://doi.org/10.1117/12.2555035

[17] Zhang, H., Liu, J., Lu, E., Suo, X., & Chen, N. (2019). A novel surface roughness measurement method based on the red and green aliasing effect. *Tribology International*, *131*, 579–590. https://doi.org/10.1016/j.triboint.2018.11.013

[18] Gorbenko, A., & Popov, V. (2012). Usage of the Laplace Transform as a Basic Algorithm of Railroad Tracks Recognition. *International Journal of Mathematical Analysis*, *6*(48), 2413–2417. http://m-hikari.com/ijma/ijma-2012/ijma-45-48-2012/popovIJMA45-48-2012.pdf

[19] Sun, B., Feng, J., & Saenko, K. (2016, March). Return of frustratingly easy domain adaptation. In *Proceedings of the AAAI Conference on Artificial Intelligence* (Vol. 30, No. 1). https://doi.org/10.1609/aaai.v30i1.10306

[20] Krizhevsky, A., Sutskever, I., & Hinton, G. E. (2017). ImageNet classification with deep convolutional neural networks. *Communications of the ACM*, *60*(6), 84–90. https://dl.acm.org/doi/abs/10.1145/3065386

[21] Chen, Y., Yi, H., Liao, C., Huang, P., & Chen, Q. (2021). Visual measurement of milling surface roughness based on Xception model with convolutional neural network. *Measurement*, *186*, 110217. https://doi.org/10.1016/j.measurement.2021.110217

[22] Wieczorowski, M., Kucharski, D., Sniatala, P., Krolczyk, G., Pawlus, P., & Gapinski, B. (2021, November). Theoretical considerations on application of artificial intelligence in coordinate metrology. In *2021 6th International Conference on Nanotechnology for Instrumentation and Measurement (NanofIM)* (pp. 1–4). IEEE. https://doi.org/10.1109/NanofIM54124.2021.9737344

[23] Pawlus, P., Reizer, R., & Wieczorowski, M. (2021). Functional importance of surface texture parameters. *Materials*, *14*(18), 5326. https://doi.org/10.3390/ma14185326

[24] Senin, N., & Leach, R. (2018). Information-rich surface metrology. *Procedia CIRP*, *75*, 19–26. https://doi.org/10.1016/j.procir.2018.05.003

[25] Zhang, F. (2018). Instantaneous cutting behavior of high energy efficiency milling cutter and its evaluation method. *Harbin University of Science and Technology*. https://kns.cnki.net/KCMS/detail/detail.aspx?dbname=CMFD201901&filename=1018173174.nh (in Chinese)

[26] Hsu, P. L., & Yang, W. T. (1993). Realtime 3D simulation of 3-axis milling using isometric projection. *Computer-Aided Design*, *25*(4), 215–224. https://doi.org/10.1016/0010-4485(93)90052-P

[27] Choi, B. K., Chung, Y. C., & Park, J. W. (1995). Application and extension of Z-map model. In *Proc. of the 3rd Pacific Conference on Computer Graphics and Applications* (pp. 363-382). https://xueshu.studiodahu.com/scholar?q=Application+and+extension+of+Z-map+model

[28] Nguyen, V., Dang, T., & Jin, F. (2018). Predict saturated thickness using TensorBoard visualization. *Workshop on Visualisation in Environmental Sciences* (EnvirVis). https://doi.org/10.2312/envirvis.20181135

[29] Vogelsang, D. C., & Erickson, B. J. (2020). Magician's corner: 6. TensorFlow and TensorBoard. *Radiology: Artificial Intelligence*, *2*(3). https://doi.org/10.1148/ryai.2020200012

[30] Liu, L., Zhang, Q., & Wei, X. (2012). A RGB image encryption algorithm based on DNA encoding and chaos map. *Computers & Electrical Engineering*, *38*(5), 1240–1248. https://doi.org/10.1016/j.compeleceng.2012.02.007

[31] Al-Jubouri, Q., Al-Azawi, R. J., Al-Taee, M., & Young, I. (2018). Efficient individual identification of zebrafish using Hue/Saturation/Value color model. *The Egyptian Journal of Aquatic Research*, *44*(4), 271–277. https://doi.org/10.1016/j.ejar.2018.11.006

Lingli Lu is a postgraduate student of the College of Mechanical and Control Engineering at Guilin University of Technology. Her main research area is machine vision.

Aihua Shu is a teacher at the College of Foreign Languages of Guilin University of Technology.

Huaian Yi is an associate professor at the College of Mechanical and Control Engineering at Guilin University of Technology. His main research area is machine vision.

Jianhua Qin is an associate professor at the College of Mechanical and Control Engineering at Guilin University of Technology. His main areas of interests are robotics, TCM information detection and processing.